Theory of fluorescence recovery after photobleaching measurements on cylindrical surfaces

David E. Wolf
Worcester Foundation for Experimental Biology, Shrewsbury, Massachusetts 01545

ABSTRACT The theory of fluorescence recovery after photobleaching measurements of isotropic diffusion on a cylindrical surface is developed for Gaussian beam illumination centered perpendicular to an infinitely-long cylinder. A general analytical solution is obtained which is a function of the ratio of the cylindrical radius (r) to the beam exp $[-2]$ radius ω. Numerical analysis of this solution demonstrates that significant deviations from one dimensional recovery are observed for $\omega < 3r$ and from two-dimensional recovery for $\omega \geq 0.5r$. Numerical data and an algorithm for analysis of recovery data where $0.5r \leq \omega \leq 3r$ is presented.

INTRODUCTION

Fluorescence recovery after photobleaching (FRAP) is a widely used technique for measuring surface diffusion of lipids and proteins in biological membranes (Axelrod, 1976; Wolf and Edidin, 1981; Wolf, 1989; Elson and Qian, 1989; Peters, 1981). While other geometries have been developed (Elson and Qian, 1989; Schulten, 1986; Koppel, 1985; Koppel and Sheetz, 1983; Koppel, 1979; Smith et al., 1979; Smith and McConnell, 1978; Lanni and Ware, 1982; Devoust et al., 1982; Sheetz et al., 1980), the most common manifestation of FRAP instrumentation, so-called "spot" FRAP, makes use of the natural Gaussian TEM_{∞} laser resonance mode, and the property of Gaussians that they remain Gaussian in the diffraction limit. In his original development of the theory of "spot" FRAP, Axelrod (1976) assumed that the membrane could be approximated by an infinite two-dimensional plane. A number of papers have extended the applicability of FRAP measurements by treating specific geometric corrections to this planar geometry and the assumption of infinite source (Elson and Qian, 1989; Petersen and McConnaughey, 1982; Aizenbud and Gershen, 1982; Wolf et al., 1982; Koppel and Sheetz, 1983; Sheetz et al., 1980).

In this paper we further extend "spot" FRAP theory to the case of diffusion on a cylindrical surface. This case is relevant, for instance, to measuring diffusion on sperm flagellae (Wolf and Voglmayr, 1984; Wolf et al., 1986) and neuronal processes (Treistman et al., 1987). While in principle one can modify instrumentation to produce a line bleach, which leads to one-dimensional recovery, this has detrimental effects on signal to noise. Furthermore, it is inconvenient when one wants to compare diffusion on sperm heads to tails, or neuronal bodies to processes, where the geometry of the two regions is different.

We present an analytical solution of this problem which is a function of the ratio of the cylindrical radius, r, to exp $[-2]$ radius of the laser beam, ω. Numerical analysis of this solution demonstrates that significant deviations from one-dimensional recovery are observed for $r/\omega > 0.3$ and from two-dimensional recovery for $r/\omega \leq 2.0$. Numerical data and an empirical algorithm are presented which facilitate analysis of FRAP data where $0.3 \leq r/\omega \leq 2.0$.

THEORY

Consider an infinitely long cylindrical membrane of radius (r) which lies along the z-axis. The membrane contains a fluorescent molecule at uniform surface concentration, C_0, which is completely free to diffuse isotropically in the membrane with a diffusion coefficient, D. The membrane is illuminated by a laser beam which is directed along the x-axis. Fig. 1 shows the cross-section within the x-y plane of both the cylinder and the laser beam. If we assume that the intensity profile does not change significantly as a function of depth, x (see Discussion), then the intensity at any point along the surface will be given by

$$\mathbf{I}(z, y) = \mathbf{I}_0 \exp\left[-2(z^2 + y^2)/\omega^2\right], \tag{1}$$

which can be written in terms of cylindrical coordinates z, r, θ as

$$\mathbf{I}(z, \theta) = \mathbf{I}_0 \exp\left[-2(z^2 + r^2 \sin^2\theta)/\omega^2\right]. \tag{2}$$

We consider first the bleaching process. Let $C[z, \theta, t]$ be the concentration of fluorophore at any point on the surface at any time. Following Axelrod (1976) we assume that the incident light bleaches the fluorescence by a first order process with rate constant α and that recovery during the bleach is negligible. That is,

$$\mathrm{d}C[z, \theta, t]/\mathrm{d}t = -\alpha \mathbf{I}[z, \theta] C[z, \theta, t]. \tag{3}$$

The solution to Eq. 3 is

$$C[z, \theta, 0] = C_0 \exp\left[-\alpha T \mathbf{I}[z, \theta]\right], \tag{4}$$

0006-3495/92/02/487/07 $2.00

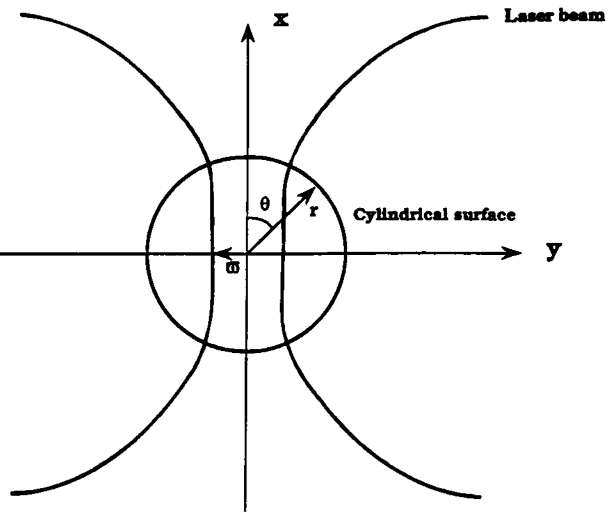

FIGURE 1. Schematic diagram showing, in cross section in the x-y plane, bleaching of a cylindrical surface of radius r, which lies along the z-axis with a Gaussian Laser beam of $\exp[-2]$ radius ω along the x-axis. We define a cylindrical coordinate system where θ is the azimuthal angle from the x-axis in the (x, y) plane.

where T is the duration of the bleach and where we have defined $t = 0$ to be at the end of the bleach.

It is convenient to define a parameter, k, a measure of the extent of bleach, as

$$k \equiv \alpha T I_0. \tag{5}$$

Therefore,

$$C[z, \theta, 0] = C_0 \exp[-k \exp[-2(z^2 + r^2 \sin^2\theta)/\omega^2]]. \tag{6}$$

The bleach establishes a concentration gradient $C[z, \theta, 0]$ which will decay back to homogeneity by random diffusion. If $C[z, \theta, t]$ is the time-dependent concentration, then the fluorescence intensity as a function of time, $F_k[t]$, is given by

$$F_k[t] = (q/A)\int_{-\infty}^{+\infty} dz \int_0^{2\pi} r d\theta I[z, \theta] C[z, \theta, t], \tag{7}$$

where q is the product of the quantum efficiencies for light absorption, emission, and detection, A is the attenuation of the monitoring beam over the bleaching beam, and $r dz\, d\theta$ is the differential area element on the surface of the cylinder in cylindrical coordinates.

$C[z, \theta, t]$ is determined by solving the diffusion equation in cylindrical coordinates. The assumption of isotropic diffusion here translates to equal axial and azimuthal diffusion coefficients. The diffusion equation is then given by

$$\partial C[z, \theta, t]/\partial t = D\partial^2 C[z, \theta, t]/\partial z^2 + (D/r^2)\partial^2 C[z, \theta, t]/\partial\theta^2. \tag{8}$$

Eq. 7 may be solved by Fourier transformation into reciprocal μ space. The Fourier transform of $C[z, \theta, t]$ is $\hat{C}[\mu_z, m, t]$ and is given by

$$\hat{C}[\mu_z, m, t] = 2^{-1/2}\pi^{-3/2}\int_{-\infty}^{+\infty} dz \int_0^{\pi} d\theta \cdot \exp[-i\mu_z z]\cos[m\theta] C[z, \theta, t]. \tag{9}$$

Putting Eq. 9 into Eq. 8 and interchanging the order of integration and differentiation one obtains

$$d\hat{C}[\mu_z, m, t]/dt = -(\mu_z^2 + m^2/r^2) D\hat{C}[\mu_z, m, t]. \tag{10}$$

The solution of Eq. 10 is

$$\hat{C}[\mu_z, m, t] = \hat{C}[\mu_z, m, 0]\exp[-(\mu_z^2 + m^2/r^2)Dt], \tag{11}$$

where $\hat{C}[\mu_z, m, 0]$ is the Fourier transform of Eq. 6.

$$\hat{C}[\mu_z, m, 0] = 2^{-1/2}\pi^{-3/2}\int_{-\infty}^{+\infty} dz \int_0^{\pi} d\theta C_0 \cdot \exp[-k\exp[-2(z^2 + r^2\sin^2\theta)/\omega^2]] \cdot \cos[m\theta]\exp[-i\mu_z z]. \tag{12}$$

To solve Eq. 12 we expand the outer exponential as a power series of the inner exponential. Thus,

$$\hat{C}[\mu_z, m, 0] = 2^{-1/2}\pi^{-3/2}\sum_{n=0}^{\infty}\int_{-\infty}^{+\infty} dz((-k)^n/n!) \cdot \exp[-2nz^2/\omega^2]\exp[-i\mu_z z] \cdot \int_0^{\pi} d\theta \exp[-2nr^2\sin^2\theta/\omega^2]\cos[m\theta]. \tag{13}$$

The z integrals are of the form

$$\int_{-\infty}^{+\infty} dx \exp[-(ax^2 + ibx)] = (\pi/a)^{1/2}\exp[-b^2/4a]. \tag{14}$$

From Eq. 13 we see that the θ integrals are 0 for odd values of m. These θ integrals can be written in terms of the modified Bessel functions $I_\nu[x]$ (Abramowitz and Stegun, 1970). For integer values of ν

$$I_\nu[x] = (1/\pi)\int_0^{\pi}\exp[x\cos\theta]\cos[\nu\theta]d\theta. \tag{15}$$

Using Eq. 14 and 15 and applying the identity

$$2\sin^2\theta = \cos 2\theta + 1, \tag{16}$$

Eq. 13 becomes

$$\hat{C}[\mu_z, m, 0] = (C_0\omega/2)\sum_{n=0}^{\infty}((-k)^n/n!n^{1/2}) \cdot \exp[-\mu_z^2\omega^2/8n]\exp[-nr^2/\omega^2] I_{m/2}[-nr^2/\omega^2]. \tag{17}$$

$C[z, \theta, t]$ can now be determined by transforming Eq. 11 back into z, θ space. Thus,

$$C[z, \theta, t] = (C_0\omega 2^{-3/2}\pi^{-1/2})\sum_{n=0}^{\infty}((-k)^n/n!n^{1/2}) \cdot \int_{-\infty}^{+\infty} d\mu_z \exp[-\mu_z^2\omega^2/8n]\exp[-\mu_z^2 Dt] \cdot \exp[+i\mu_z z]\sum_{m=-\infty}^{+\infty}\exp[-nr^2/\omega^2] I_m[nr^2/\omega^2] \cdot \cos[m\theta]\exp[-m^2Dt/r^2]. \tag{18}$$

In Eq. 18 we have made use of the symmetry of $I_m[x]$ about 0 and the fact that m was even to redefine m as $m/2$ enabling us to sum over all rather than only even m values.

The integral in μ_z can be solved using Eq. 14 where $a = \omega^2/8n + Dt$ and $b = z$. Thus, Eq. 18 becomes

$$C[z, 0, t] = (C_0\omega 2^{-3/2}) \sum_{n=0}^{\infty} ((-k)^n/n!n^{1/2}) \cdot \{\exp[-z^2/4(\omega^2/8n + Dt)]/(\omega^2/8n + Dt)^{1/2}\} \cdot \sum_{m=-\infty}^{+\infty} \exp[-nr^2/\omega^2]I_m[nr^2/\omega^2] \cos[m\theta] \exp[-m^2Dt/r^2]. \quad (19)$$

Eq. 19 must then be put into Eq. 7 to solve for $F_k[t]$.

$$F_k[t] = (q/A)C_0\omega 2^{-3/2}\,\mathbf{I}_0 \sum_{n=0}^{\infty}\sum_{m=-\infty}^{+\infty} \cdot \{((-k)^n/n!n^{1/2}) \exp[-nr^2/\omega^2]I_m[nr^2/\omega^2] \cdot \exp[-m^2Dt/r^2]\}/(\omega^2/8n + Dt)^{1/2} \cdot \int_{-\infty}^{+\infty} dz \exp[-z^2/4(\omega^2/8n + Dt)] \exp[-2z^2/\omega^2] \cdot \int_0^{2\pi} r d\theta \exp[-2r^2 \sin^2\theta/\omega^2] \cos[m\theta]. \quad (20)$$

The z integral is again of the form of Eq. 14 and the θ integral can again be expressed in terms of the modified Bessel functions. Eq. 20 thus becomes

$$F_k[t] = (q/A)(C_0 2^{-1/2}\pi^{3/2}\omega r\mathbf{I}_0) \sum_{n=0}^{\infty}\sum_{m=-\infty}^{+\infty}\{((-k)^n/n!) \cdot \exp[-(n+1)r^2/\omega^2]I_m[r^2/\omega^2]I_m[nr^2/\omega^2] \cdot \exp[-m^2Dt/r^2]\}/((\omega^2/8n + Dt) \cdot (2/\omega^2 + \tfrac{1}{4}(\omega^2/8n + Dt)n^{1/2})$$

$$= (q/A)C_0(2^{1/2})\pi^{3/2}\omega r I_o \sum_{n=0}^{\infty} ((-k)^n/n!)/ (1 + n(1 + 8Dt/\omega^2))^{1/2} \cdot \sum_{m=-\infty}^{+\infty} \exp[-(n+1)r^2/\omega] \cdot \exp[-m^2Dt/r^2]I_m[r^2/\omega^2]I_m[nr^2/\omega^2]. \quad (21)$$

Making the substitution $\tau_D = \omega^2/4D$ Eq. 21 becomes

$$F_k(t) = (q/A)C_0(2^{1/2})\pi^{3/2}\omega r\mathbf{I}_0 \sum_{n=0}^{\infty} \cdot ((-k)^n/n!)/(1 + n(1 + 2t/\tau_D))^{1/2} \cdot \sum_{m=-\infty}^{+\infty} \exp[-(n+1)r^2/\omega^2] \cdot \exp[-m^2(\omega^2/r^2)(t/\tau_D)/4]I_m[r^2/\omega^2]I_m[nr^2/\omega^2]. \quad (22)$$

If we apply the symmetry condition that $I_m[nr^2/\omega^2] = I_{-m}[nr^2/\omega^2]$, Eq. 22 becomes

$$F_k(t) = (q/A)C_0(2^{1/2})\pi^{3/2}\omega r\mathbf{I}_0 \sum_{n=0}^{\infty} ((-k)^n/n!)/ (1 + n(1 + 2t/\tau_D))^{1/2} \cdot \exp[-(n+1)r^2/\omega^2] \cdot \exp[-m^2(\omega^2/r^2)(t/\tau_D)/4)]\Big\{I_0[r^2/\omega^2]I_0[nr^2/\omega^2] + 2\sum_{m=1}^{\infty} I_m[r^2/\omega^2]I_m[nr^2/\omega^2]\Big\}. \quad (23)$$

Limit $r/\omega \to 0$

In the limit $r/\omega \to 0$ we expect $F_k(t)$ to become the one-dimensional solution. In this limit, we have

$$\exp[-m^2(\omega^2/r^2)(t/\tau_D)/4] \to 1 \text{ for } m = 0, \quad \to 0 \text{ for } m > 0$$

and $\exp[-(n+1)r^2/\omega^2] \to 1$ for all n. Thus,

$$F_k(t) = (q/A)C_0(2^{1/2})\pi^{3/2}\omega r\mathbf{I}_0 I_0^2[0] \cdot \sum_{n=0}^{\infty} ((-k)^n/n!)/(1 + n(1 + 2t/\tau_D))^{1/2}. \quad (24)$$

Recognizing that $I_0[0] = 1$ and defining the density per unit length to be $\sigma = C_0 2\pi r$, we see that Eq. 24 is indeed the solution for one-dimensional recovery (Koppel, 1985).

$$F_k(t) = (q/A)(\sigma(\pi/2)^{1/2})\omega\mathbf{I}_0 \cdot \sum_{n=0}^{\infty} ((-k)^n/n!)/(1 + n(1 + 2t/\tau_D))^{1/2}. \quad (25)$$

Limit $r/\omega \to \infty$

In the limit $r/\omega \to \infty$ we expect $F_k(t)$ to become the two-dimensional solution. This is most readily seen by reconsidering the θ integral in Eq. 13. As $r/\omega \to \infty$ the argument in the exponential $-2nr^2 \sin^2\theta/\omega^2$ is large for all n except when θ is small. Thus, $\sin^2\theta$ can be approximated by θ^2 and the limit 2π replaced by ∞. Since m is even, $\cos[m\theta]$ can be replaced with $\exp[im\theta]$ without loss of generality, and the subsequent sum over m in Eq. 18 replaced with an integral over m. Thus, the solution for the two variables z and θ become symmetric and $F_k[t]$ becomes

$$F_k[t] = (q/A)C_0(\pi/2)\omega^2\mathbf{I}_0 \sum_{n=0}^{\infty} \cdot ((-k)^n/n!)/(1 + n(1 + 2t/\tau_D)), \quad (26)$$

which is the case for two-dimensional recovery (Axelrod, 1976).

Limit $t \to 0$

In the limit $t \to 0$ we expect $F_k[t]$ to become $F_k[0]$ as defined by Eq. 6. In this limit Eq. 23 becomes

$$F_k[0] = (q/A)C_0(2^{1/2})\pi^{3/2}\omega r\mathbf{I}_0 \sum_{n=0}^{\infty} ((-k)^n/n!)/(1 + n)^{1/2} \cdot \exp[-(n+1)r^2/\omega^2](I_0[r^2/\omega^2]I_0[nr^2/\omega^2] + 2\sum_{m=1}^{\infty} I_m[r^2/\omega^2]I_m[nr^2/\omega^2]). \quad (27)$$

The same result can be obtained by putting Eq. 6 into Eq. 7.

$$F_k[0] = (q/A)C_0\mathrm{I}_0 \int_{-\infty}^{+\infty} \mathrm{d}z \int_0^{2\pi} r\mathrm{d}\theta \exp\left[-2(z^2 + r^2 \sin^2\theta)/\omega^2\right] \cdot \exp\left[-k \exp\left[-2(z^2 + r^2 \sin^2\theta)\right]\right]. \quad (28)$$

To solve this equation we again expand the double exponential term.

$$F_k[0] = (q/A)C_0\mathrm{I}_0 \sum_{n=0}^{\infty} ((-k)^n/n!) \int_{-\infty}^{+\infty} \mathrm{d}z \exp\left[-2(n+1)z^2/\omega^2\right] \cdot \exp - \left[(n+1)r^2/4\omega^2\right] \int_0^{2\pi} r \,\mathrm{d}\,\theta \cdot \exp[r^2 \cos 2\theta/\omega^2] \exp\left[nr^2 \cos 2\theta/\omega^2\right]. \quad (29)$$

Upon application of the identity (Abramowitz and Stegun, 1970)

$$\exp\left[x \cos\theta\right] = I_0[x] + 2 \sum_{m=1}^{\infty} I_m[x] \cos m\theta \quad (30)$$

Eq. 29 becomes Eq. 27.

NUMERICAL ANALYSIS

Eq. 23 was numerically evaluated for different values of r/ω using Mathematica (Wolfram Research Association, Champaign, IL) on a Northgate 386 computer with Math Coprocessor. Diffusion problems of this kind have their weakest convergence where $(\omega^2/r^2)(t/\tau_D)$ is small (Sommerfeld, 1949) and where k is large. Thus, one might anticipate problems when $t = 0$, r/ω becomes large, and k is large. To test convergence of Eq. 23, we independently evaluated $F_k[0]$ by numerical integration of Eq. 27. Allowing n to run from 0 to 100 and m to run from 0 to 15 resulted in less than a 0.2% discrepancy between these two solutions. Additionally, the solutions converge appropriately (Figs. 2 and 3) to the one-dimensional case as $r/\omega \rightarrow 0$ and to the two-dimensional case as $r/\omega \rightarrow \infty$.

Fig. 2 shows recovery curves for 70% bleach for representative values of r/ω ranging from 0 to ∞. We see that for $r/\omega = 0.3$ there is little difference from one-dimensional diffusion while for $r/\omega = 2.0$ there is little difference from two-dimensional diffusion.

Axelrod (1976) proposed a three point method of analysis of FRAP curves based upon a theoretical determination of the ratio of the halftime for recovery to τ_D, referred to as γ, as a function of $F[0]$. While some laboratories directly fit experimental data to the power series solution, many nonlinear curve fitting algorithms for FRAP analysis do not fit directly, but rely instead upon an empirical data fit which is then connected to theory using γ tables (Barisas and Leuther, 1977; Wolf and Edidin, 1981; Wolf, 1989). γ values appropriate for the different r/ω values at 70% bleach can be found from Fig. 2 by determining the value of t/τ_D at which the recovery curves reach $F = 0.65$. The inset to Fig. 2 shows the correction factors $\gamma_{r/\omega}/\gamma_{1D}$ and $\gamma_{r/\omega}/\gamma_{2D}$ as a function of r/ω to such a γ analysis for 70% bleach to the assumptions of either one- or two-dimensional recovery.

Generation of tables of $\gamma_{r/\omega}$ vs. $F[0]$ is computationally intensive. We therefore suggest an equally valid approach to determining diffusion coefficients from FRAP recovery curves on cylinders. For a given case of r/ω, one uses Eq. 23 to determine as a function of k, $F[0]$, and $F[1]$. This gives us a table or plot of $F[1]$ vs. $F[0]$. For an experimental recovery curve with some $F[0]$, we then determine at what time the recovery reaches $F[1]$. This will occur at $t = \tau_D$. D can then be determined from $D = \omega^2/4\tau_D$. Operationally, because in real FRAP curves there is an immobile fraction, it is most useful to determine the fraction of this recovery observed at $t = \tau_D$ namely $(F[1] - F[0])/(1 - F[0])$. If the mobile fraction is f, then the actual recovery observed at $t = \tau_D$ will be $f(F[1] - F[0])/(1 - F[0])$.

Fig. 3 shows calculated values of $(F[1] - F[0])/(1 - F[0])$ as a function of $F[0]$ for different values of r/ω. These plots can be used as described to determine D for a given value of r/ω. Once again we see that serious deviation from one-dimensional solutions is observed in the range $0.3 < r/\omega < 2.0$.

DISCUSSION

In developing this solution we have assumed that the beam radius does not change significantly with depth, x. If there were significant variations with depth, Eq. 1 would need to be replaced with (Elson and Qian, 1989):

$$\mathrm{I}(x, y, z) = [\mathrm{I}_0\omega_0^2/\omega^2(x)] \exp\left[-2(z^2 + y^2)/\omega^2(x)\right] \quad (31)$$

which would considerably complicate the analysis. We must, therefore, consider the validity of this assumption. When focussed, the actual waist (radius $= \omega_0$) of the beam will be at $x = 0$ and the dependence of radius $\omega[x]$ on x will be given by (Elson and Qian, 1989).

$$\omega^2[x] = \omega_0^2[1 + (\lambda x/n\pi\omega_0^2)^2], \quad (32)$$

where λ is the wavelength, say 0.5 μ, and n is the index of refraction of the medium, say 1.3. If we consider the extreme case of $x = 2\omega_0$, that is $r/\omega = 2$, we find

$$\omega^2[2\omega_0] = \omega_0^2[1 + (1.3\pi\omega_0)^2] = \omega_0^2 + (1.3/\pi)^2. \quad (33)$$

For the typical case of $\omega_0 = 1$ μm, $\omega[2\omega_0] = 1.03$. Thus, for the case of $r/\omega = 2.0$ we can expect about a 3% variation in radius as a function of depth. Smaller variations will be found for smaller values of r/ω. This

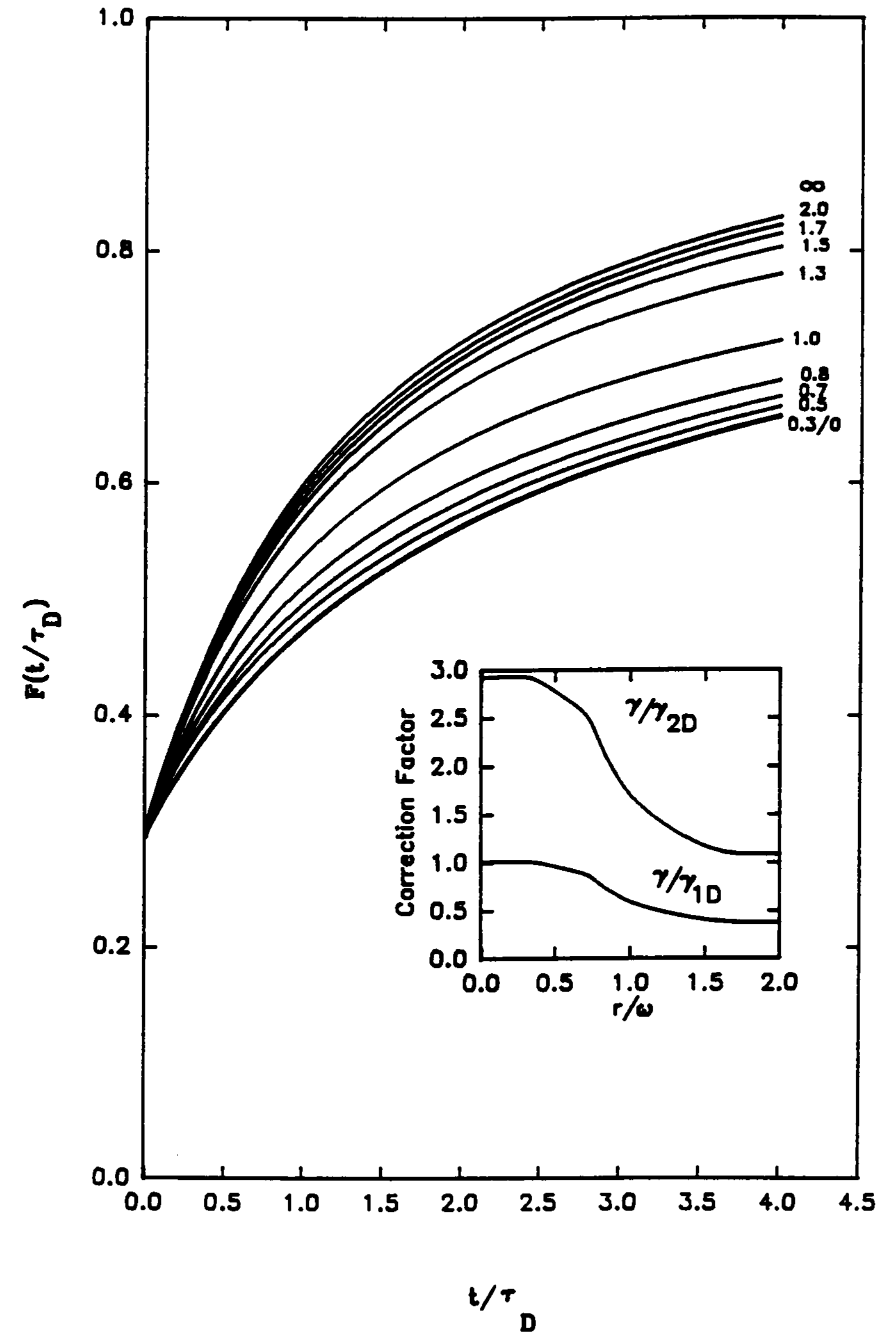

FIGURE 2. FRAP recovery curves for 70% bleach (i.e., $F[0] = 0.3$) as a function of normalized time t/τ_D for different values of r/ω. γ is the value of t/τ_D for half recovery (i.e., $F[t_{1/2}/\tau_D] = 0.65$). The inset shows multiplicative correction factors for the different r/ω values, to one- ($r/\omega = 0$) and two- ($r/\omega = \infty$) dimensional recovery. Curves were generated using Eq. 23 for r/ω from 0.3 to 2.0, Eq. 25 for $r/\omega = 0$, and Eq. 26 for $r/\omega = \infty$.

variation is small compared to typical uncertainties of 10 to 20% in measured values of ω_0 (Schneider and Webb, 1981). Thus, for practical purposes, the solution (Eq. 23) is valid for the range of r/ω where correction is necessary.

It is also of interest to consider the applicability of Eq. 23 to biological problems. Consider, for instance, diffusion on the mid-piece of mammalian spermatozoa. Mammalian sperm heads are so small that one would need to use a laser beam with an $\omega \sim 0.5$ to 1.0 μm.

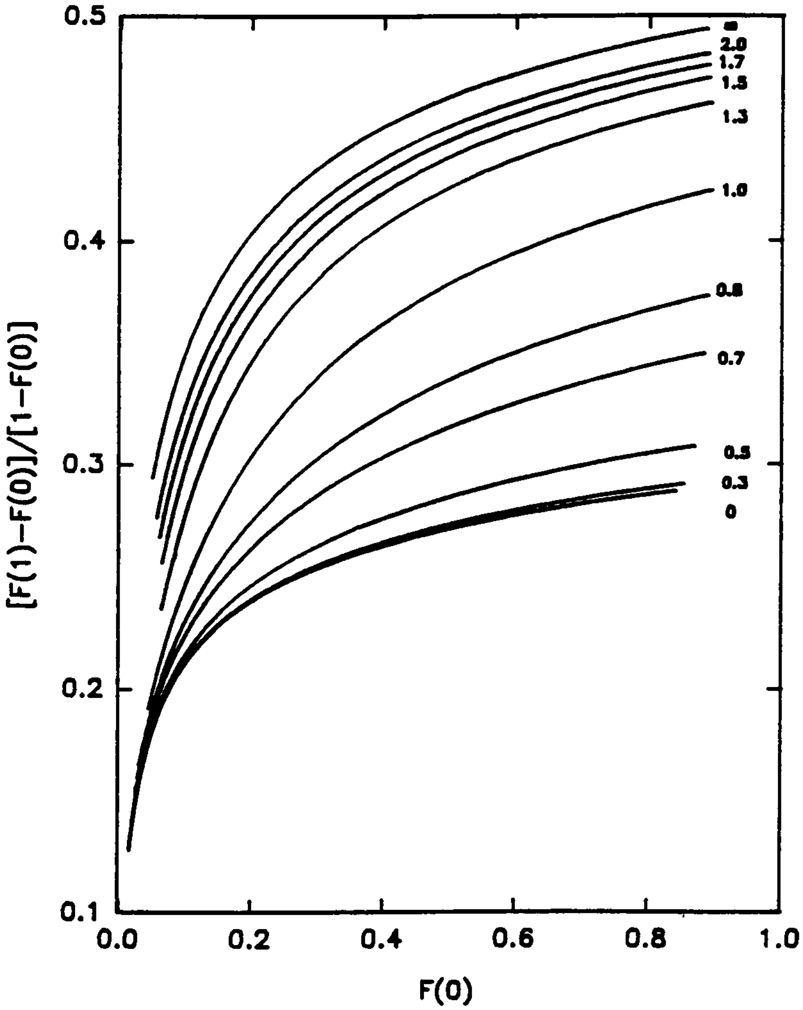

FIGURE 3. The fractional recovery at $t/\tau_D = 1$, $(F[1] - F[0])/(1 - F[0])$ as a function of unbleach fraction $F[0]$ for the different values of r/ω. Curves were generated using Eq. 23 for r/ω from 0.3 to 2.0, Eq. 25 for $r/\omega = 0$, and Eq. 26 for $r/\omega = \infty$. As described in the text, this data enables determination of diffusion coefficients from recovery data.

Using the same beam on the midpiece where r values dependent upon species range from ~0.3 to 1.0 μm (Cardullo and Wolf, 1990), corresponds to r/ω ranging from ~0.3 to 2.0 which is the range considered here. When $r/\omega \simeq 1.0$, we see from Fig. 2 that incorrect use of either the one- or two-dimensional γ tables would result in about a twofold error in the diffusion coefficient. Eq. 23 is equally applicable to neuronal and other cellular processes. Indeed, the considerable variability and tapering of such processes accentuate the need for such a correction if accurate determinations of diffusion coefficients are to be made.

On a practical level one can conclude that if $r/\omega > 2$ the two-dimensional solution can be used, while if $r/\omega \leq 0.3$ the one-dimensional solution can be used. In the intermediate range, Eq. 23 must be applied. For typical ω values of 0.5 to 1.0 μm, the condition $r/\omega \leq 0.3$ translates to $r \leq 0.15$ to 0.30 μm. Because the resolution of the light microscope is in the same range, the lower limit leads to an empirical rule that the correction must be applied if one can resolve the cylindrical thickness.

The author wishes to thank James Christo, Richard Cardullo, Dennis Koppel, and Christine McKinnon for help in the preparation of this manuscript. Numerical analysis was performed using Mathematica (Wolfram Research, Inc.).

This work was supported in part by NIH grant HD-17377 and by grants from the Whitaker and A.W. Mellon Foundations.

Received for publication 9 April 1991 and in final form 27 September 1991.

REFERENCES

Aizenbud, B. M., and N. D. Gershon. 1982. Diffusion of molecules on biological membranes of nonplanar form a theoretical study. *Biophys. J.* 38:287–294.

Abramowitz, M., and I. Stegnun. 1970. Handbook of mathematical functions. United States Government Printing Office, Washington, DC. p. 376.

Axelrod, D., D. E. Koppel, J. Schlessinger, E. L. Elson, and W. W. Webb. 1976. Mobility measurements by analysis of fluorescence photobleaching recovery kinetics. *Biophys. J.* 16:1055–1069.

Barisas, B. G., and M. D. Leuther. 1977. Fluorescence photobleaching recovery measurement of protein absolute diffusion coefficients. *Biophys. Chem.* 10:221–229.

Cardullo, R. A., and D. E. Wolf. 1990. The sperm plasma membrane—a little more than mosaic, a little less than fluid. *In* Ciliary and Flagellar Membranes. R. A. Bloodgood, editor. Plenum Press, NY. 305–336.

Devoust, J., P. F. DeVaux, and L. Leger. 1982. Fringe pattern photobleaching, a new method for the measurement of transport coefficients of biological macromolecules. *EMBO J.* 1:1233–1238.

Elson, E. L., and H. Qian. 1989. Interpretation of fluorescence correlation spectroscopy and photobleaching in terms of molecular interactions. *In* Methods in Cell Biology, Vol. 30, D. L. Taylor and Y.-l. Wang, editors. Academic Press, NY. 307–332.

Koppel, D. E. 1979. Fluorescence redistribution after photobleaching. A new multipoint analysis of membrane translational dynamics. *Biophys. J.* 28:281–292.

Koppel, D. E. 1985. Normal-mode analysis of lateral diffusion on a banded membrane surface. *Biophys. J.* 47:337–347.

Koppel, D. E., and M. P. Sheetz. 1983. A localized pattern photobleaching method for the concurrent analysis of rapid and slow diffusion processes. *Biophys. J.* 43:175–181.

Lanni, F., and B. R. Ware. 1982. Modulation detection of fluorescence photobleaching recovery. *Rev. Sci. Instrum.* 53:905–908.

Peters, R. 1981. Translational diffusion in the plasma membrane of single cells as studied by fluorescence microphotolysis. *Cell Biol. Internatl. Rep.* 5:733–760.

Petersen, N. O., and W. B. McConnaughey. 1982. Effects of multiple membranes on measurements of cell surface dynamics by fluorescence photobleaching. *J. Supramol. Struct. Cell Biochem.* 17:213–222.

Schulten, K. 1986. Continuous fluorescence microphotolysis by a Sin2KX grating. *Chem. Phys. Lett.* 124:230–236.

Schneider, M. B., and W. W. Webb. 1981. Measurement of sub-micron laser beam radii. *Appl. Opt.* 20:1382–1388.

Sheetz, M. P., M. Schindler, and D. E. Koppel. 1980. Lateral mobility of integral membrane protein is increased in spherocytic erythrocytes. Nature (*Lond.*). 258:510–512.

Smith, B. A., and H. M. McConnell. 1978. Determination of molecular motions in membranes using periodic pattern photobleaching. *Proc. Natl. Acad. Sci. USA.* 75:2759–2763.

Smith, B. A., W. R. Clark, and H. M. McConnell. 1979. Anisotropic molecular motion on cell surfaces. *Proc. Natl. Acad. Sci. USA.* 76:5641–5644.

Somerfeld A. 1949. Partial differential equations in physics. Academic Press, New York. 71–74.

Treistman, S., M. M. Moynihan, and D. E. Wolf. 1987. Influence of alcohols, temperature, and region on the mobility of lipids in neuronal membranes. *Biochem. Biophys. Acta.* 898:109–120.

Wolf, D. E., and M. Edidin. 1981. Diffusion and mobility in surface membranes. *In* Techniques in Cellular Physiology. P. Baker, editor. Elsevier, North Holland. 105:1–14.

Wolf, D. E., and J. K. Voglmayr. 1984. Diffusion and regionalization in membranes of maturing ram spermatozoa. *J. Cell Biol.* 98:1678–1684.

Wolf, D. E. 1989. Designing, building, and using a fluorescence recovery after photobleaching instrument. *In* Methods in Cell Biology, Vol. 30. D. L. Taylor and Y.-l. Wang, editors. Academic Press, New York. 271–332.

Wolf, D. E., S. S. Hagopian, and S. Ishijima. 1986. Changes in sperm plasma membrane lipid diffusibility after hyperactivation during in vitro capacitation in the mouse. *J. Cell Biol.* 102:1372–1377.

Wolf, D. E., A. H. Handyside, and M. Edidin. 1982. Effect of microvilli on lateral diffusion measurements made by the fluorescence photobleaching recovery technique. *Biophys. J.* 38:295–298.